Coaxial Antenna Slot Impact On Thermal Effectiveness In Microwave Ablation Therapy

4 authors:

Olumide Adewole Towoju
Adeleke University
23 PUBLICATIONS 22 CITATIONS

SEE PROFILE

Timilehin Fiyin Sanni
Covenant University Ota Ogun State, Nigeria
18 PUBLICATIONS 17 CITATIONS

SEE PROFILE

Felix Ishola
Covenant University Ota Ogun State, Nigeria
43 PUBLICATIONS 43 CITATIONS

SEE PROFILE

Soji-Adekunle Rita
Adeleke University
1 PUBLICATION 1 CITATION

SEE PROFILE

Some of the authors of this publication are also working on these related projects:

Energy Management View project

Performance characterization of CI engines View project

Coaxial Antenna Slot Impact On Thermal Effectiveness In Microwave Ablation Therapy

Olumide A. Towoju, Felix A. Ishola, Timilehin Sanni, Rita Soji-Adekunle

Abstract: Ablation is a minimally invasive procedure used in the treatment of small tumours. Tumour sizes of about 3 cm are now been effectively treated with thermal ablation therapy using either microwave ablation or radiofrequency ablation. The impact of the slot position on a coaxial antenna on the extent of thermal lesion at the tumour site was investigated numerically in this study by varying the slot distance from the antenna tip using COMSOL Multiphysics as the modelling tool. The coaxial antenna size investigated has a diameter of 1.79 mm, with a central conductor diameter of 0.29 mm and Tefzel ETFE as the catheter material. The coaxial antenna performance was optimized at a slot distance of 6 mm from the antenna tip. The total power dissipation density and hence, the degree of thermal lesion created during the procedure is dependent on slot position of the coaxial antenna.

Index Terms: Catheter, Coaxial antenna, Microwave Ablation, Necrosis, Thermal lesion, Temperature distribution, Tumour.

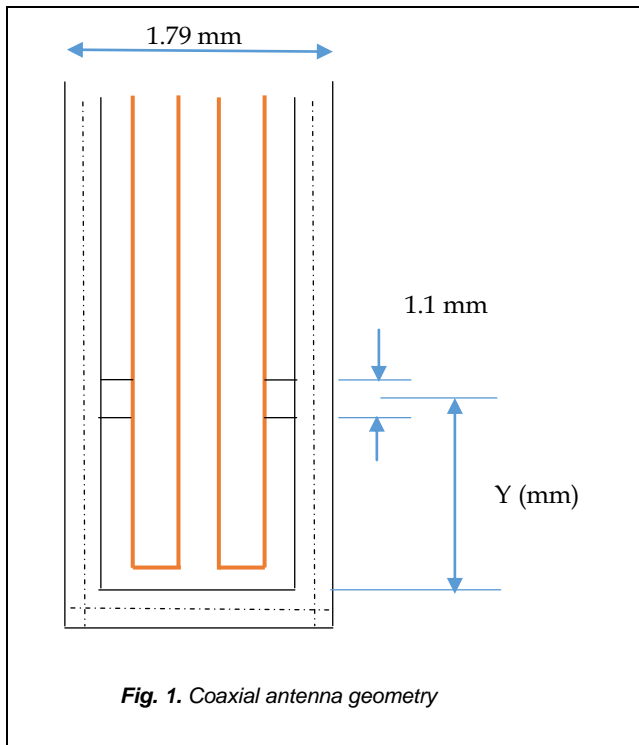————————————————◆————————————————

1 INTRODUCTION

Ablation, a minimally invasive procedure is now being commonly used in the treatment of small tumours in human organs that span from the liver, kidney, pancreas, breast, and even the heart [1], especially in cases where surgery is not a good option. Ablation is best used for tumour sizes below 7 cm, and for optimum results, it works well for tumour sizes of about 3 cm [2], [3]. While the microwave ablation (MWA) and the radiofrequency ablation (RFA) are the commonly utilized heat ablation procedures, ethanol ablation and cryotherapy are also gaining grounds. Microwave ablation (MWA) and radiofrequency ablation (RFA) achieve necrosis using thermal energy developed by the probe which is inserted by any of the three means; through surgery, percutaneously, or by laparoscopy procedure using image guidance. However, while microwave ablation utilizes high frequency microwave to achieve thermal lesion, radiofrequency ablation uses alternating radiofrequency current to achieve lesion [3], [4], [5] ,6]. Ethanol ablation achieves necrosis by the direct injection of concentrated alcohol as against the use of heat, and is usually applied only when tumours are very small and defiles other techniques of treatment like in hepatocellular cancer, while cryotherapy achieves necrosis through very low temperature caused by the passage of cold gases through the probe to the tumour site, and is effective of larger tumour sizes than the other ablation techniques [3], [5]. In the treatment of kidney cancer, the morbidity rate and complication rates are lower with the use of thermal ablation than with the use of partial nephrectomy, however, the cancer specific mortality rate is still a major advantage of nephrectomy [7], [8], [9]. The less dependence of microwave ablation on tissue electrical conductivity and its reliability at higher intra-tumour temperatures makes it a better efficient procedure in the treatment of tumours of larger size than the radiofrequency ablation procedure [10], [11], [12], [13]. The offering of a hope to patients who are not compliable to surgery coupled with the reduced recovery period, cost, and the possibility of

application in cases of multiple tumour sites of renal microwave ablation has made it to be a viable alternative to partial nephrectomy [12], [13], [14], [15], [16], [17], [18], [19]. Improved image guidance technology has also in no small way made microwave ablation safer and more effective in the treatment of renal tumour [20], [21], even as it has helped in other areas of surgery [22]. Microwave ablation therapy is less painful procedurally in comparison to the other ablation techniques, and also offers the advantages of high intra-tumour temperatures and faster ablation time [18], [23], [24]. It uses electromagnetic radiations in form of short pulses [25] usually with frequencies of either 915 MHz or 2.45 GHz to ensure thermal lesion of the tumour [18], [26], [27], [28], [29]. The propagation of the microwave determines the degree of thermal lesion caused during microwave ablation, this is related to the intensity, time duration, geometry of the antenna, and the tissue relative permittivity [14], [28], [30], [31], [32]. Several antenna geometry types have been studied like the co-axial based and sleeve, and the geometry is made such as to be minimally invasive and efficient [30], [33], [34], [35], [36], [37]. The efficiency being a function of the Specific Absorption Ratio (SAR). Asides the antenna geometry, the catheter material properties are also a contributor to the level of necrosis that can be achieved during microwave ablation [38]. This study is focused on the temperature distribution of the antenna as a function of the slot position in microwave ablation, as the tissue necrosis is dependent on the prevailing temperature. Temperatures of over 42^0C are usually considered to be lethal to human cells [14], [40], [41].

2 METHODOLOGY

The numerical model follows the cancer microwave therapy developed by COMSOL Multiphysics [39] for a coaxial slot antenna geometry. Radiofrequency and heat transfer modules were employed in carrying out the modelling of the liver ablation zone caused by the antenna. The catheter material employed for the conduct of this work was Tefzel ETFE based on the earlier findings of it having properties that favours greater degree of thermal lesion [38]. The modelled antenna geometry is depicted in Figure 1.

——————————————————

- *Olumide A. Towoju is currently a lecturer at Mechanical Engineering Department, Adeleke University, Ede, Nigeria. PH. +2348055934207 E-mail: olumidetowo@yahoo.com*
- *Felix A. Ishola is currently a lecturer at Mechanical Engineering Department, Covenant University, Ota, Nigeria. E-mail: felix.ishola@covenantuniversity.edu.ng*
- *Timilehin Sanni is currently a lecturer at Electrical and Information Engineering, Department, Covenant University, Ota, Nigeria.*
- *Rita Soji-Adekunle is currently a lecturer at Mechanical Engineering Department, Adeleke University, Ede, Nigeria*

Fig. 1. Coaxial antenna geometry

The interior of the metallic conductors is not modelled, however, the metallic parts are modelled using boundary conditions by setting the tangential component of the electric field to zero.

A temperature of $37\,°C$ was used for blood, and a frequency of 2.45 GHz was used for the antenna operation.

The numerical modelling was carried out in Two-dimension axisymmetric coordinate, taking advantage of the problem's rotational symmetry.

The governing equations for the electromagnetic wave propagation in the coaxial cable which is characterized by transverse electromagnetic fields are;

$$E_\tau = e_r \frac{C}{r} e^{j(\omega t - kz)} \tag{1}$$

$$H_\tau = e_\varphi \frac{C}{z} e^{j(\omega t - kz)} \tag{2}$$

$$Z = e_z \pi \frac{C^2}{P_{ab}} In\left(\frac{r_{out}}{r_{in}}\right) \tag{3}$$

where r_{in} is the inner radius of dielectric material, r_{out} is the outer radius of dielectric material, Z is the dielectric wave impedance, ω is the angular frequency, P_{ab} is the power input, while, r, φ, and z are the cylindrical coordinates.

The wave number which is the propagation constant "k" = $\frac{\omega}{v}$, and since V = fλ, and $\omega = 2\pi f$, therefore, the propagation constant expressed as a function of the wavelength (medium) as;

$$k = \frac{2\pi}{\lambda} \tag{4}$$

Using a low-reflecting boundary condition, the antenna is modelled using the axisymmetric transverse magnetic formulation, since in the tissue, the electric field has a finite axial component and the magnetic field is purely in azimuthal direction.

$$nx\sqrt{\varepsilon E} - \sqrt{\mu H_\varphi} = -2\sqrt{\mu H_{\varphi 0}} \tag{5}$$

The bio-heat equation governs the time-dependent heat transfer, neglecting the heat from metabolism, it is stated as;

$$\rho C_p \frac{\partial T}{\partial t} + \nabla.(-k\nabla T) = \rho_{bld} C_{bld} \omega_{bld}(T_{bld} - T) + Q_{ext} \tag{6}$$

where T_{bld} is the temperature of blood, ω_{bld} is the blood perfusion rate, k is the thermal conductivity of tissue, Q_{ext} is the external heat source which is equal to the resistive heat generated by the electromagnetic field, C_{bld} is blood specific heat capacity, and ρ_{bld} is the blood density.

The necrotic tissue fraction is derived from the expression;

$$\emptyset_d = 1 - \text{exponential}(-\alpha) \tag{7}$$

where the tissue injury degree "α" is based on the Arrhenius equation;

$$\frac{d\alpha}{dt} = F_f \exp\left(\frac{-dE}{RT}\right) \tag{8}$$

F_f is the frequency factor, dE is the activation energy of the irreversible damage.

The material properties utilized for the simulation is depicted in Table 1, Table 2 shows the geometry of the antenna, and Table 3 depicts the properties of blood.

The impact of slot size and position on the thermal distribution of the antenna were then investigated numerically using a microwave generator of 10 W with an application time of 15 minutes.

TABLE 1
PROPERTIES OF MATERIALS

Material	Relative permittivity	Conductivity (S/m)
Liver	43.03	1.69
Inner dielectric	2.03	
Tefzel ETFE	2.311	

TABLE 2
ANTENNA DIMENSIONS

Property	Value (mm)
Central conductor diameter	0.290
Outer conductor inner diameter	0.940
Outer conductor outer diameter	1.190
Catheter diameter	1.790

TABLE 3
PROPERTIES OF BLOOD

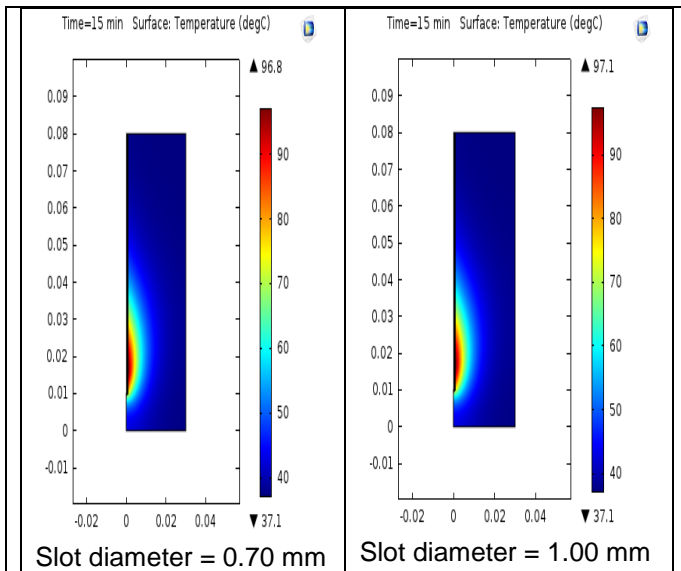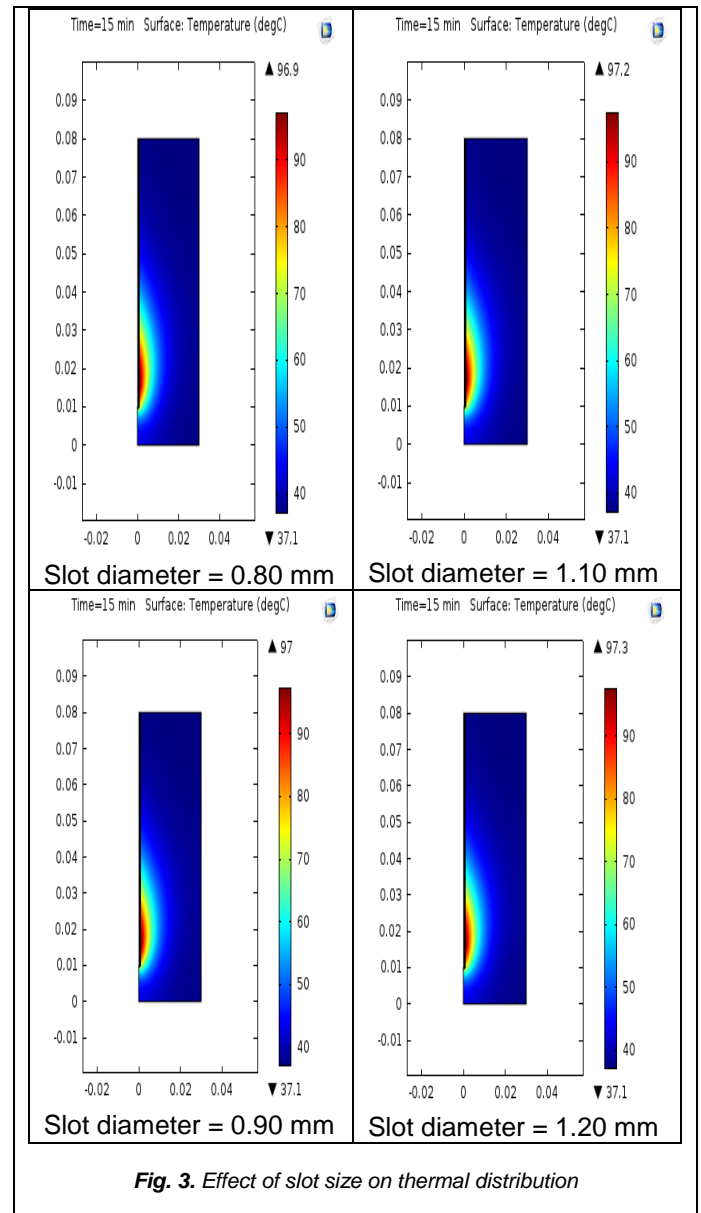| Parameter	Value
Temperature (^{0}C)	37
Density (kg/m^3)	1045
Perfusion rate (1/s)	0.0036
Specific heat (J/kg K)	3639

3 RESULTS AND DISCUSSIONS

3.1 Effect of Coaxial Antenna Slot Size

The size of the slot was observed to be a determinant of the fraction of the input power absorbed by the tissue. The tissue absorbed power is utilized in its heating which eventually causes thermal lesion. Figure 2 shows the total power dissipation density for different slot diameters at a distance 'y' = 4 mm from the antenna tip. The larger the slot diameter, the greater the fraction of the input power that is absorbed by the tissue, and since the efficiency of the antenna is dependent on the total power dissipation density, a larger slot diameter is

31

favoured, however, this will be limited by the outer conductor outer and inner diameters.

Fig. 2. *Total power dissipation density dependency on slot diameter*
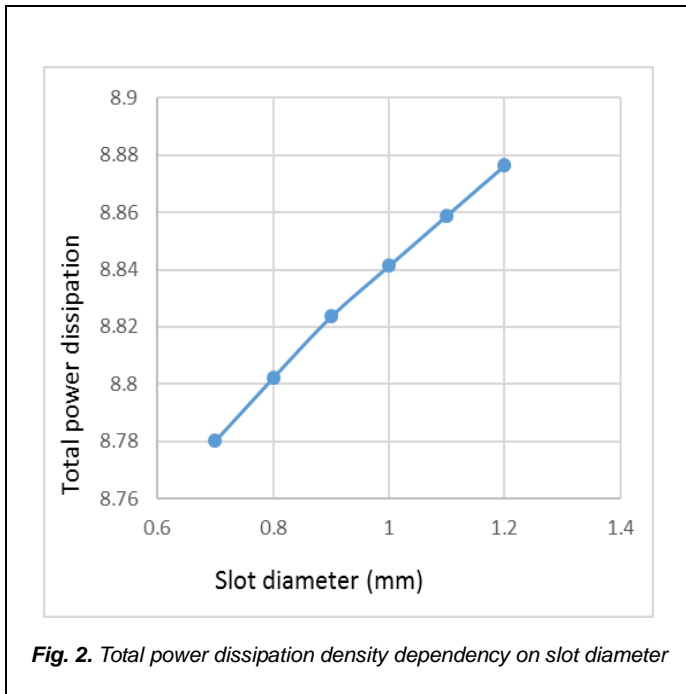
With the outer conductor diameter of 1.190 mm as stated in Table 2, the largest slot diameter that can be used is 1.10 mm, and this is what was utilized in the simulation to determine the impact of the slot position 'y' on the thermal properties of the coaxial antenna. Figure 3 shows the thermal distribution in the tissue for the different antenna slot diameters. The peak temperature attained by the antenna is dependent on the slot size, with a larger sized slot favouring higher temperature distributions.

Slot diameter = 0.70 mm   Slot diameter = 1.00 mm

Slot diameter = 0.80 mm   Slot diameter = 1.10 mm

Slot diameter = 0.90 mm   Slot diameter = 1.20 mm

Fig. 3. *Effect of slot size on thermal distribution*

3.2 Effect of The Use of Tapered Slot

The results of the impact of tapered slot located at a distance 'y' = 4 mm on the total power dissipation density and thermal properties are shown in Figure 4, for both inward tapered and outward tapered with 1.10 mm as the base diameter in all cases. The tapered slot in all investigated cases led to improved power absorption by the tissue in comparison to the equivalent un-tapered slot but with diameter equal to that of the tapered end. The inward tapered slot geometry despite having the same dimensions with the outward tapered slot geometry resulted into improved power absorption by the tissue.
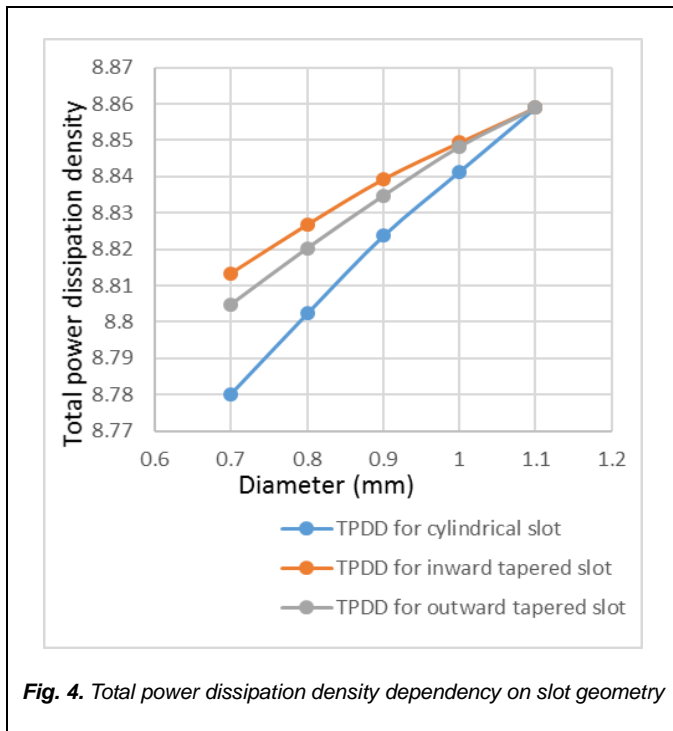
Fig. 4. *Total power dissipation density dependency on slot geometry*

3.2 Coaxial Antenna Slot Location Effect

The total power dissipation density was observed to be a function of the slot position, that is, its location from the antenna tip. Figure 5 is the plot of total power dissipation density versus slot location from the coaxial antenna tip for a slot size of 1.10 mm diameter. The fraction of the power absorbed by the tissue increased as the slot position from the antenna tip increases, however at a distance 'y' = 6 mm, the absorbed power was a maximum, and the subsequent increase in distance from the tip antenna led to a reduction in the absorbed power.
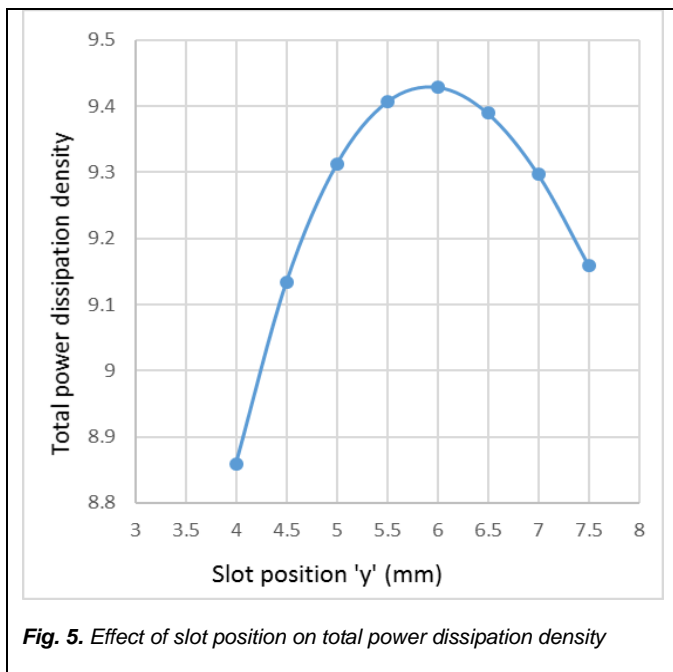

Fig. 5. *Effect of slot position on total power dissipation density*

The temperature distribution in the tissue determines the necrosis of the tissue, is dependent on the absorbed input power, and is therefore dependent on the slot position. Figures 6 and 7 shows the temperature distribution and the fraction of tissue necrosis achieved for the different coaxial slot positions respectively.
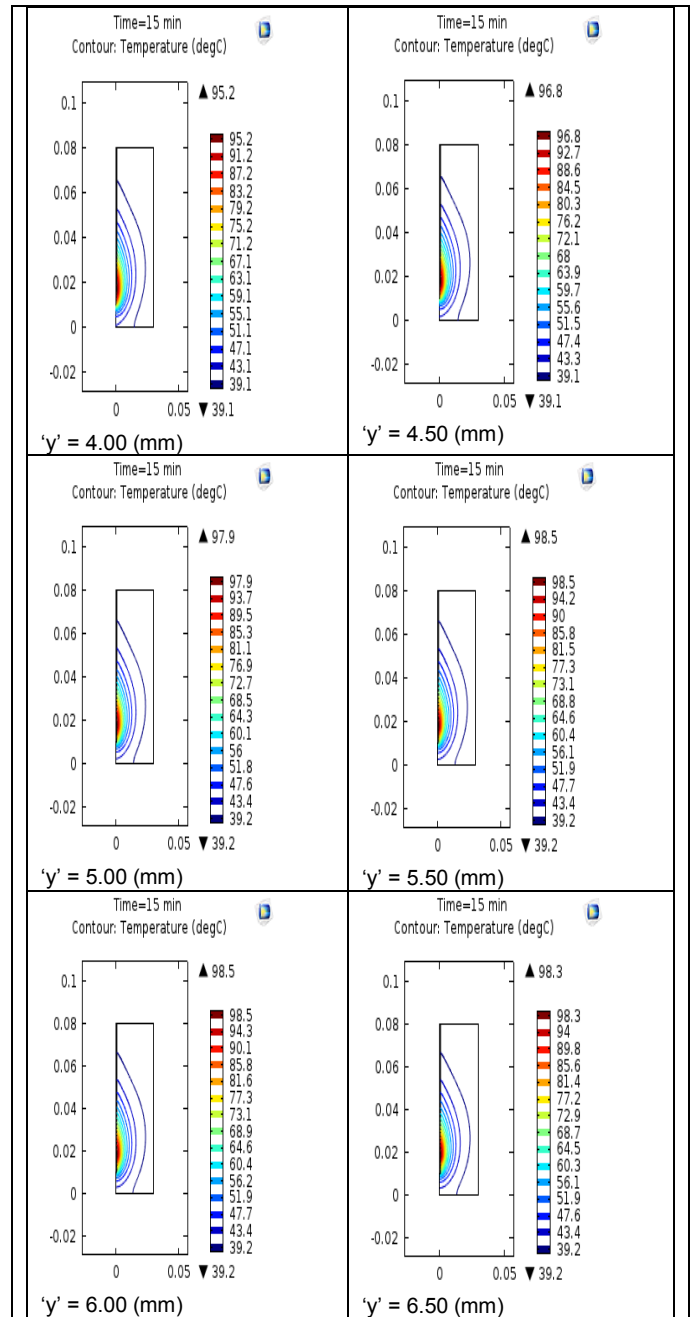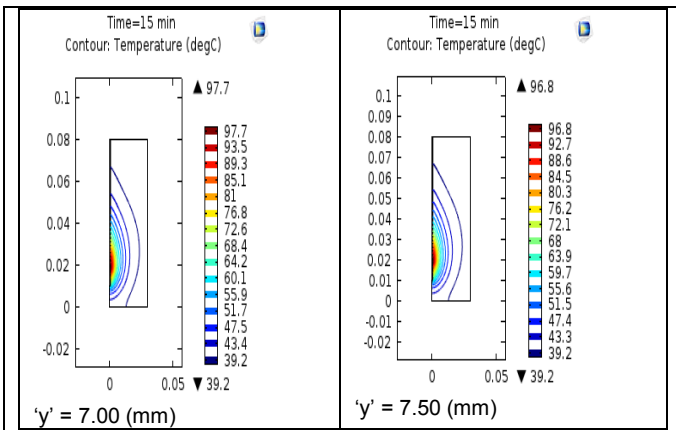
Fig. 6. *Thermal properties of the tissue relationship with slot position*
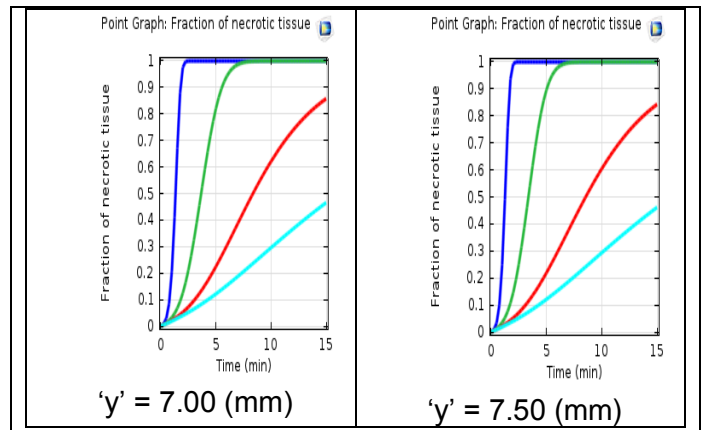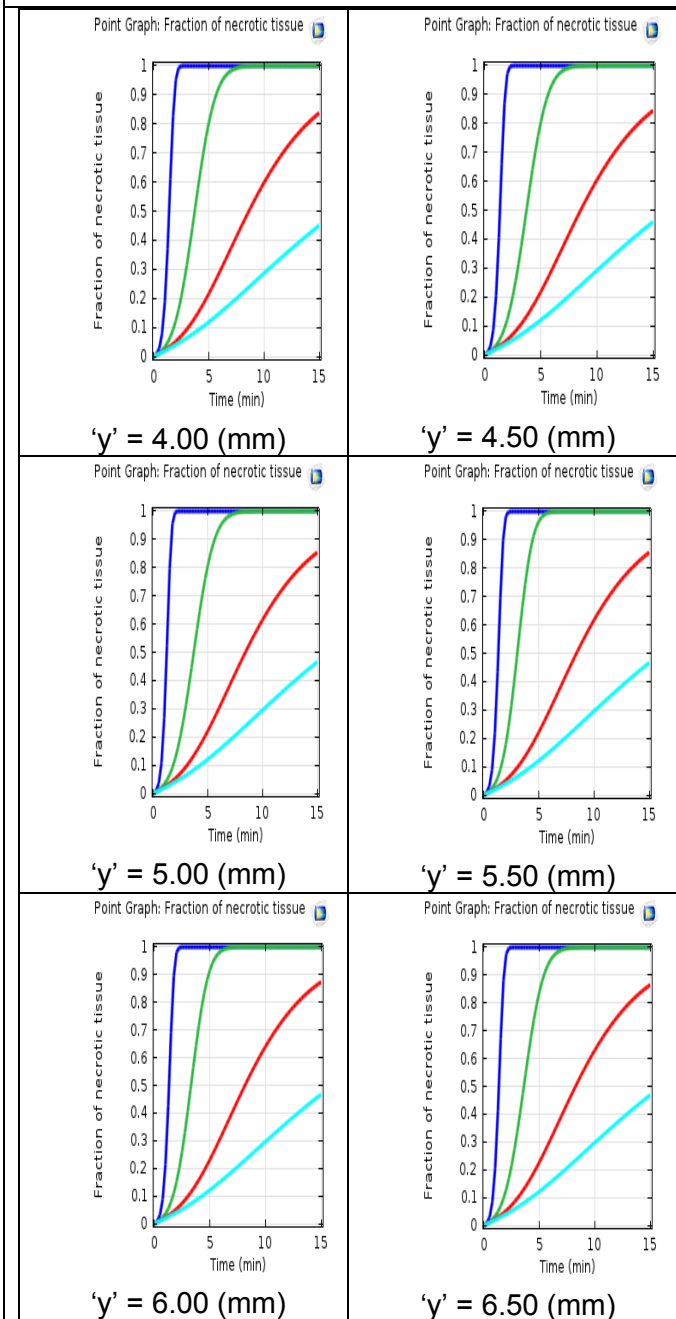

Fig. 7. *Effect of necrotic tissue fraction on slot position*

The fraction of necrotic tissue at a radii position 1.5 mm from the coaxial antenna axis which connotes a 3 mm diameter spherical ablation zone was observed to be maximum at a slot position 'y' = 6 mm in agreement with the slot position that had the maximum absorbed input power, and it is also the position of peak temperature distribution values. The model can be used to predict the effect of slot diameter located at distance 'y' = 4mm from the coaxial antenna tip, and the slot position for a slot diameter of 1.1 mm respectively on the total power dissipation density using regression analysis. The models are depicted in Figures 8 and 9 respectively.
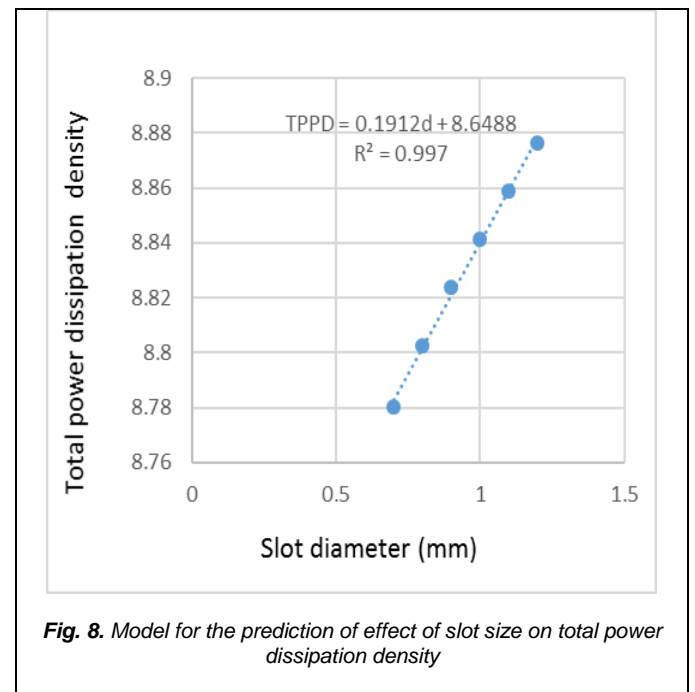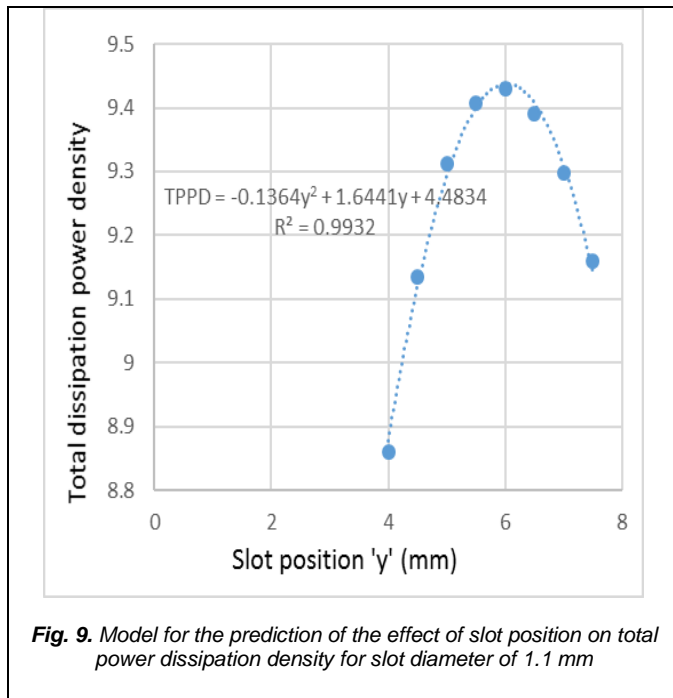

Fig. 8. *Model for the prediction of effect of slot size on total power dissipation density*

Fig. 9. *Model for the prediction of the effect of slot position on total power dissipation density for slot diameter of 1.1 mm*

For the effect of slot size, the linear equation;

$$TPDD = 0.1912d + 8.6488 \qquad (9)$$

is applicable where TPDD is the total power dissipation density, and d is the slot diameter in mm, is the model equation, while the effect of the slot position from the coaxial antenna tip on the total power dissipation density is governed by the quadratic equation;

$$TPDD = -0.1364y^2 + 1.6441y + 4.4834 \qquad (10)$$

The 'R squared' value for the two model are very close to '1', an indication that the predictions made with the model will be very close to the real values, making them a reliable predictive tool.

4 CONCLUSION

A correlation exists between the total power dissipation density, temperature distribution in the tissue and the fraction of the necrotic tissue. the following observations were deduced from the numerical investigation;

   i. The coaxial antenna slot size has a direct relationship with the total power dissipation density and hence, the tissue necrosis which is a function of the temperature.
   ii. The temperature distribution of the antenna in the tissue is a function of the slot geometry, with the inward tapered slot geometry showing better performance than the outward tapered slot geometry.
   iii. The slot position from the coaxial antenna tip is a determinant of its total power dissipation density and temperature distribution, and a distance 'y' exist at which the performance of the antenna is optimized, and for this studies it was at 6 mm.

REFERENCES
[1] S. Ribar, M. Dramićanin, T. Dramićanin, L. Matija, "Classification of Breast Cancer Organizing Luminescence Data Using Self-Mapping Neural Network," FME Transactions, vol. 34, pp. 87-91, 2006.
[2] S. C. Campbell, A. C. Novick, A. Belldegrun, M. L. Blute, et al., "Guideline for Management of the Clinical T1 Renal Mass," J Urol, vol. 182, pp. 1271-1279, 2009.
[3] https://www.cancer.org/cancer/liver-cancer/treating/tumor-ablation.html accessed on 30/09/2018
[4] https://www.radiologyinfo.org/en/info.cfm?pg=rfaliver accessed on 04/10/2018
[5] https://www.hopkinsmedicine.org/liver_tumor_center/treatments/ablative_techniques/microwave_ablation.html accessed on 04/10/2018
[6] https://www.cancerresearchuk.org/about-cancer/lung-cancer/treatment/microwave-ablation accessed on 30/09/2018
[7] J. R. Rivero JoseDe, L. CerdaIII, H. Wang, M. A. Liss, A. M. Farrell, R. Rodriguez, R. Suri, and D. Kaushik, "Partial Nephrectomy versus Thermal Ablation for Clinical Stage T1 Renal Masses: Systematic Review and Meta-Analysis of More than 3,900 Patients," Journal of Vascular and Interventional Radiology, vol. 29, no. 1, pp. 18-29, 2018.
[8] S. E. McAchranO. A. Lesani, and M. I. Resnick, "Radiofrequency ablation of renal tumors: Past, present, and future, Urology, vol. 66, no. 5, pp. 15-22, 2005.
[9] S. N. Goldberg, G. S. Gazelle, and P. R. Mueller, "Thermal Ablation Therapy for Focal Malignancy: A Unified Approach to Underlying Principles, Techniques, and Diagnostic Imaging Guidance" AJR, vol. 174, pp. 323-331, 2000.
[10] S. P. Psutka, A. S. Feldman, W. S. McDougal, F. J. McGovern, P. Mueller, and D. A. Gervais, "Long-term Oncologic Outcomes after Radiofrequency Ablation for T1 Renal Cell Carcinoma," Eur Urol, vol. 63, pp. 486-492, 2013.
[11] O. Seror, "Ablative Therapies: Advantages and Disadvantages of Radiofrequency, Cryotherapy, Microwave and Electroporation Methods, or How to Choose the Right Method for an Individual Patient?" Diagnostics and Interventional Imaging, vol. 96, pp. 617-624, 2015.
[12] J. Yu, P. Liang, X. Yu, F. Liu, L. Chen, and Y. Wang, "A Comparison of Microwave Ablation and Bipolar Radiofrequency Ablation both with an Internally Cooled Probe: Results in Ex Vivo and in Vivo Porcine Livers," European Journal of Radiology, vol. 79, pp. 124-130, 2011.
[13] F. Cornelis, P. Balageas, Y. Le Bras, G. Rigou, Boutault, J-R., M. Bouzgarrou, and N. Grenier, "Radiologically-guided Thermal Ablation of Renal Tumors," Diagnostics and Interventional Imaging, vol. 93, pp. 246-261, 2012.
[14] F. H. Cornelis, C. Marcelin, and J. C. Bernhard, "Microwave Ablation of Renal Tumors: A Narrative Review of Technical Considerations and Clinical Results," Diagnostics and Interventional Imaging, vol. 98, pp. 287-297, 2017.

[15] G. C. Hui, K. Tuncali, S. Tatli, P. R. Morrison, and S. G. Siverman, "Comparison of Percutaneous and Surgical Approaches to Renal Tumors Ablation," J Vasc Interv Radiol., vol. 19, no. 9, pp. 1311-1320, 2008.

[16] S. L. Woldu, G. R. Thoreson, Z. Okhunov, R. Ghandour, M. B. Rothberg, A. RoyChoudhury, H. H. Kin, M. Bozoghlanian, J. H. Newhouse, M. A. Helmy, K. K. Badana, J. Landman, J. A. Cadeddu, and J. M. McKieman, "Comparison of Renal Parenchymal Volume Preservation Between Partial Nephrectomy, Croablation, and Radiofrequency Ablation Using 3D Volume Measurements," J Endourol., vol. 29, no. 8, pp. 948-955, 2015.

[17] J. A. Long, J. C. Bernhard, C. Pigot, "Partial Nephrectomy versus Ablative Therapy for the Treatment of Renal Tumors in an Imperative Setting," World J Urol, vol. 35, pp. 649-656, 2016.

[18] C. Floridi, L. De Bernardi, F. Fontana, "Microwave Ablation of Renal Tumors: State of the Art and Development Trends," Radiol Med, vol. 119, pp. 533-540, 2014.

[19] T. J. Vogl, N. N. Naguib, T. Lehnert, and N. A. Nour-Eldin, "Radiofrequency, Microwave and Laser Ablation of Pulmonary Neoplasms: Clinical Studies and Technical Considerations – Review Article," European Journal of Radiology, vol. 77, pp. 346-357, 2011.

[20] P. L. Yang, W. D. Zhang, X. Yu Yongyan, and G. Xiaoxia Ni, "Ultrasound Guided Percutaneous Microwave Ablation for Small Renal Cancer: Initial Experience," J Urol, vol. 180, no. 3, pp. 844-848, 2008.

[21] L. J. Higgins and K. Hong, "Renal Ablation Techniques: State of the Art.," AJR, vol. 205, pp. 735-741, 2015.

[22] M. Sljvic, M. Stanojevic, D. Djurdjevic, N. Grujovic, and A. Paviovic, "Implemenation of FEM and Rapid Prototyping in Maxillofacial Surgery," FME Transactions, vol. 44, pp. 422-429, 2016.

[23] S. M. Castle, N. Salas, and R. J. Leveillee, "Initial Experience Using Microwave Ablation Therapy for Renal Tumor Treatment: 18-Month Follow-up, Urology," vol. 77, no. 4, pp. 792-797, 2011.

[24] C. J. Simon, D. E. Dupuy, and W. W. Mayo-Smith, "Microwave Ablation: Principles and Applications", Radiographics, vol. 25, pp. 69-83, 2005.

[25] B. M. Radojković, S. S. Ristić, and S. R. Polić-Radovanović, "Study of Ruby Laser Beam Interaction with Glass," FME Transactions, vol. 41, pp. 109-113, 2013.

[26] G. Deshazer, P. Prakash, D. Merck, and D. Haemmerich, "Experimental Measurement of Microwave Ablation Heating and Comparison to Computer Simulations," Int J Hyperthermia, vol. 33, pp. 74-82, 2017.

[27] C. L. Brace, "Radiofrequency and Microwave Ablation of the Liver, Lung, Kidney and Bone: What are the Differences," Curr Probl Diagn Radiol, vol. 38 no. 3, pp. 135-143, 2009.

[28] C. L. Brace, "Microwave Tissue Ablation: Biophysics, Technology and Applications," Crit RevBiomed Eng., vol. 38, no. 1, pp. 65-78, 2010.

[29] T. Baere and F. Deschamps. "New Tumors Ablation Techniques for Cancer Treatment (Microwave, Electroporation)," Diagnostic and Interventional Imaging, vol. 95, pp. 677-682, 2014.

[30] P. Prakash, "Theoretical Modeling for Hepatic Microwave Ablation," The Open Biomedical Engineering Journal, vol. 4, pp. 27-38, 2010.

[31] G. L. DeNardo and S. J. DeNardo. "Turning the Heat on Cancer," Cancer Biotherapy & Radiopharmaceuticals, vol. 23, no. 6, pp. 671-679, 2008.

[32] A. M. Lerardi, A. Mangano, C. Floridi, G. Dionigi, et al., "A New System of Microwave Ablation at 2450 MHz: Preliminary Experience," Updates Surg, vol. 67, pp. 39-45, 2015.

[33] J. M. Bertram, D. Yang, M. C. Converse, J. G. Webster and D. M. Mahvi. "Antenna Design for Microwave Hepatic Ablation Using Axisymmetric Electromagnetic Model," BioMedical Engineering Online, vol. 5, no. 15, pp. 1-9, 2006.

[34] A. Z. Ibitoye, T. Orotoye, E. O. Nwoye, and M. A. Aweda, "Analysis of Efficiency of Different Antennas for Microwave Ablation Using Simulation and Experimental Methods," Egyptian Journal of Basic and Applied Sciences, vol. 5, pp. 24-30, 2018.

[35] G. Schaller, J. Erb, and R. Engelbrecht, "Field Simulation of Dipole Antennas for Interstitial Microwave Hyperthermia," IEEE Transactions. Microwave Theory and Techniques, vol. 44, no. 6, pp. 887-895, 1996.

[36] C. L. Brace, D. W. Van der Weide, F. T. Lee, P. F. Laeseke, and L. Sampson, "Analysis and Experimental Validation of Triaxial Antenna for Microwave Ablation," IEEE MTTS. Int Microw Symp, vol. 3, no. (6-11), pp. 1437-1440, 2004.

[37] C. L. Brace, "Microwave Ablation Technology: What Every Use Should Know," Curr Probl Daign Radiol. vol. 38, no. 2, pp. 61-67, 2010.

[38] O. A. Towoju and M. O. Petinrin, "Thermal Lesion of Renal Tumour as a Function of Catheter Material Property," European Journal of Engineering Research and Science, vol. 3, no. 9, pp. 12-17, 2018.

[39] COMSOL (2014), "Microwave_cancer_therapy" COMSOL 5.0 (Build: 202).

[40] A. Bettaeib and D. A. Averill-Bates, "Thermotolerance Induced at a Mild Temperature 40°C Alleviates Heat Shock-Induced ER Stress and Apoptosis in HeLa Cells," Biochimica et Biophysica Acta, vol. 1853, pp. 52-62, 2015.

[41] E. R. Cosman Jr. and E. R. Cosman Sr., "Electric and Thermal Field Effects in Tissue around Radiofrequency Electrodes," American Academy of Pain Medicine, vol. 6, pp. 405-424, 2005.